Impact of the coxsackie and adenovirus receptor (CAR) on glioma cell growth and invasion: Requirement for the C-terminal domain

ARTICLE *in* INTERNATIONAL JOURNAL OF CANCER · FEBRUARY 2005

Impact Factor: 5.09 · DOI: 10.1002/ijc.20623 · Source: PubMed

8 AUTHORS, INCLUDING:

Meric Altinoz

36 PUBLICATIONS **228** CITATIONS

SEE PROFILE

Nancy Larochelle

McGill University

21 PUBLICATIONS **438** CITATIONS

SEE PROFILE

Josephine Nalbantoglu

McGill University

142 PUBLICATIONS **5,177** CITATIONS

SEE PROFILE

Int. J. Cancer: **113,** 738–745 (2005)

Impact of the coxsackie and adenovirus receptor (CAR) on glioma cell growth and invasion: Requirement for the C-terminal domain

Kuo-Cheng Huang, Meric Altinoz, Karolina Wosik, Nancy Larochelle, Zafiro Koty, Lixia Zhu, Paul C. Holland and Josephine Nalbantoglu*

Department of Neurology and Neurosurgery, McGill University and the Montreal Neurological Institute, Montreal, Quebec, Canada

Expression of the coxsackie and adenovirus receptor (CAR) is downregulated in malignant glioma cell lines and is barely detectable in high-grade primary astrocytoma (glioblastoma multiforme). We determined the effect of forced CAR expression on the invasion and growth of the human glioma cell line U87-MG, which does not express any CAR. Although retrovirally mediated expression of full-length CAR in U87-MG cells did not affect monolayer growth *in vitro*, it did reduce glioma cell invasion in a 3-dimensional spheroid model. Furthermore, in xenograft experiments, intracerebral implantation of glioma cells expressing full-length CAR resulted in tumors with a significantly reduced volume compared to tumors generated by control vector-transduced U87-MG cells. In contrast, U87-MG cells expressing transmembrane CAR with a deletion of the entire cytoplasmic domain (except for the first 2 intracellular juxtamembrane cysteine amino acids) had rates of invasion and tumor growth that were similar to those of the control cells. This difference in behavior between the 2 forms of CAR was not due to improper cell surface localization of the cytoplasmically deleted CAR as determined by comparable immunostaining of unpermeabilized cells, equivalent adenoviral transduction of the cells and similar extent of fractionation into lipid-rich domains. Taken together, these results suggest that the decrease or loss of CAR expression in malignant glioma may confer a selective advantage in growth and invasion to these tumors.

Key words: coxsackie and adenovirus receptor; glioma; spheroid; invasion; intracerebral

The coxsackie and adenovirus receptor (CAR) is the primary high-affinity receptor for adenovirus group C,[1,2] which includes the Ad 5 serotype, the most commonly used adenoviral vector (AdV) for gene transfer in cancer. The CAR protein, a member of the immunoglobulin (Ig) superfamily, with its 2 extracellular Ig-like domains, is a component of tight junctions of polarized epithelial cells,[3] the target cell of wild-type adenovirus. Although the cytoplasmic domain of CAR is dispensable for adenovirus infection,[4–11] its sequence is highly conserved between species;[2,12] it contains putative tyrosine phosphorylation sites and it may play a role in protein-protein associations through the presence of a potential PDZ (PSD95/dlg/ZO-1) interaction motif (Ser-Ile-Val [SIV] or Thr-Thr-Val [TTV]) in the described CAR isoforms. CAR can also mediate homophilic cell adhesion,[13,14] a function that may be most important during embryonic development, the period during which CAR expression is highest in most tissues.[15,16]

In cancer gene therapy, the levels of CAR and Arg-Gly-Asp (RGD)-binding integrins are the main determinants for efficient adenoviral gene transfer. However, tumor cells differ significantly from normal tissue, and between themselves, in CAR expression. This has been demonstrated in cell lines and primary tumor tissue from bladder cancer,[17] head and neck cancer,[18] lung and pancreatic cancer[19] and melanoma.[20] Absent or reduced expression of CAR is associated with higher tumor grade in human prostate and bladder cancer specimens, while the normal tissue counterparts express easily detectable levels of CAR.[21,22] As with other cancers, malignant gliomas exhibit differential levels of CAR expression that correlate directly with the efficiency of adenoviral infection.[23–25] As well, expression of CAR is downregulated in malignant glioma cell lines[24,26] and is barely detectable in high-grade primary astrocytomas (grade IV tumors or glioblastoma multiforme).[27]

A possible explanation for the reduced expression of CAR in malignant cells may be that CAR levels are governed by the activity of the Raf-MEK-ERK pathway, which is frequently deregulated in cancer. In a recent study, activation of Raf-1 resulted in decreased CAR expression, and conversely, inhibition of ERK led to increased accumulation of cell surface CAR and concomitant susceptibility to adenoviral infection.[28] Furthermore, forced expression of CAR has been found to result in inhibition of tumor cell growth in human prostate,[22,29] bladder cancer[17,21] and glioma cell lines,[30] suggesting a tumor inhibitory property of CAR. However, the biologic relevance of the forced expression of a cell-cell adhesion molecule (CAM) such as CAR needs to be considered in terms of the expression levels achieved, as well as the growth environment of the tumor. In this report we examined the effect of CAR, expressed at levels equivalent to those found in the developing brain, on the growth of an orthotopic glioma tumor model. Our results indicate that CAR expression inhibits invasion and intracerebral growth of the U87-MG glioma cell line and that this effect requires the C-terminal cytoplasmic domain.

Material and methods

Cell lines and culture conditions

The human glioma cell line U87-MG was obtained from the American Type Culture Collection (Rockville, MD). The retroviruses carrying the full-length mCAR1 isoform (CAR-LNCX) and truncated CAR (nucleotides 1–781 of mCAR1) (CAR781-LNCX) (Fig. 1) were described previously.[8] The transgenes were under the control of the cytomegalovirus (CMV) promoter. The retroviruses also expressed a neomycin phosphotransferase gene to allow the selection of stably transduced cells with geneticin (G418 sulfate). A third retrovirus containing only the neomycin resistance gene was used as the control (LNCX). The supernatants from the producer cell lines were used to transduce U87 cells, which were then selected for 10 days with G418 (600 μg/ml). The elimination of the nontransduced cells was ensured by the absence of colonies in a control nontransduced cell plate treated with G418. Clones were pooled together to generate bulk populations stably expressing the full-length mCAR1 (U87CAR), the truncated CAR (U87CAR-tailless) and the control transduced cells expressing no CAR (U87LNCX).

Cells were maintained (unless stated otherwise) at 37°C with 5% CO_2 in DMEM supplemented with 2 mM L-glutamine, 10%

Abbreviations: AdV, adenoviral vector; CAM, cell adhesion molecule; CAR, coxsackie and adenovirus receptor; CMV, cytomegalovirus; ERK, extracellular signal regulated kinase; GPI, glycosyl phosphatidylinositol; Ig, immunoglobulin; MEK, mitogen-activated protein kinase; MMP, matrix metalloprotease; MOI, multiplicity of infection; NCAM, neural cell adhesion molecule; OD, optic density; PDZ, PSD95/dlg/ZO-1; RGD, Arg-Gly-Asp; TIMP, tissue inhibitor of metalloprotease; XTT, 2,3-bis[2-methoxy-4-nitro-5-sulfophenyl]2*H*-tetrazolium-5-carboxanilide.

Grant sponsor: National Cancer Institute of Canada and the Canadian Institutes for Health Research; Grant sponsor: FRSQ-FCAR.

***Correspondence to:** Montreal Neurological Institute, 3801 University St., Montreal, Quebec, Canada H3A 2B4. Fax: +514-398-7371.
E-mail: josephine.nalbantoglu@mcgill.ca

Received 5 April 2004; Accepted after revision 28 July 2004
DOI 10.1002/ijc.20623
Published online 21 October 2004 in Wiley InterScience (www.interscience.wiley.com).

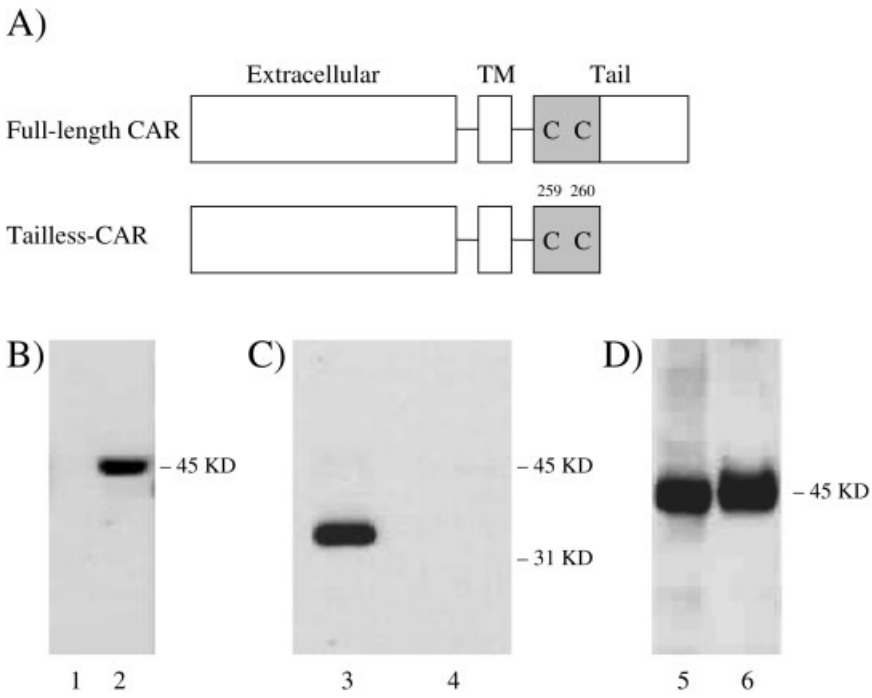

FIGURE 1 – Forced expression of CAR in U87-MG glioma cells. *(a)* Schematic depiction of the constructs used in the study. The full-length CAR construct contains an N-terminal extracellular domain, a single-pass transmembrane domain (TM) and a C-terminal cytoplasmic tail (Tail). The tailless CAR construct has the entire cytoplasmic domain deleted except for the first 2 cysteine-cysteine residues next to the transmembrane domain. *(b–d)* Western blot analysis of CAR expression with the anti-CAR N-terminal antibody (ab2240) comparing whole cell lysates of U87LNCX (*b*, lane 1; *c*, lane 4), U87CAR (*b*, lane 2; *d*, lane 5) and U87CAR-tailless (*c*, lane 3) with total brain homogenate from a P6 mouse (*d*, lane 6). Size markers are indicated on the left side of the blots. Note that while no detectable CAR was found in the U87LNCX cells, the P6 mouse brain homogenate and U87CAR cells contained equivalent levels of CAR *(d)*.

heat-inactivated FBS and an antibiotic cocktail (final concentration of 30 μg/ml gentamicin, 100 units of penicillin/ml and 100 μg of streptomycin/ml).

For cell proliferation assays, 2,500 cells of the different transduced U87 cell populations were seeded in microtiter plates (tissue culture grade, 96 wells, flat bottom) in a final volume of 200 μl of serum-supplemented medium (standard DMEM with 10% FBS) or serum-reduced medium (DMEM with 0.2% FBS) in a humidified atmosphere at 37°C and 5% CO_2. At 24, 48, 72, 96, 120 and 148 hr postplating, proliferation was assessed by a colorimetric assay with the dye (2,3-bis[2-methoxy-4-nitro-5-sulfophenyl]2*H*-tetrazolium-5-carboxanilide) sodium salt (XTT; Sigma, St. Louis, MO). Spectrophotometric absorbance of the samples was measured as optic density (OD) using a microtiter plate reader (EAR400AT, SLT-Lab Instrument, Austria) at wavelength of 450 nm. Three independent experiments were performed for each of the 3 U87 cell populations under both serum-supplemented and serum-reduced conditions. In each experiment, quadruplicate wells were analyzed at each time point.

Susceptibility to adenoviral transduction was determined as described previously[8] using an AdV that expresses the *Escherichia coli* β-galactosidase gene (AdVlacZ).

Antibodies, Western blotting and indirect immunofluorescence

The production, purification and characterization of the polyclonal antibody (ab2240) against the CAR N-terminal extracellular domain have been described in detail previously.[8] The rabbit polyclonal raised against the C-terminal intracellular domain of the human 46 kD CAR isoform (RP291) that cross-reacts with the mouse homolog mCAR1 was a kind gift of Dr. Kerstin Sollerbrant (Ludwig Institute for Cancer Research, Stockholm Branch, Karolinska Institutet, Stockholm, Sweden). Monoclonal antibody against caveolin-1 (clone 2297) was purchased from BD Biosciences Canada (Mississauga, ON). Horse radish peroxidase (HRP)-conjugated secondary antibodies were bought from DAKO Diagnostics Canada (Mississauga, ON). Alexa fluor 555-conjugated secondary antibodies were bought from Molecular Probes, Inc. (Eugene, OR).

For Western blot analysis, cells grown in monolayer culture were washed twice in ice-cold PBS and lysed in SDS-loading buffer (2% SDS, 10% glycerol, 0.125 M TRIS-HCl, pH 6.8, one tablet of complete, mini, EDTA-free protease inhibitor cocktail per 10 ml of loading buffer). The lysates were heated for 7 min at 100°C and the concentration of total protein was determined by the bicinchoninic acid (BCA) protein assay. Protein samples (10 μg/lane) were electrophoresed on a 10% polyacrylamide-SDS gel under reduced conditions (5% mercaptoethanol). Proteins on the gel were then transferred onto a nitrocellulose membrane at 100 V for 1 hr in a mini-transblot II apparatus (Bio-Rad) using a transfer buffer of 25 mM TRIS, 192 mM glycine and 20% methanol, pH 8.3. The membranes were then blocked with 5% (w/v) skim milk in TBS-T buffer (20 mM TRIS-HCl, pH 7.6, 0.14 M NaCl, 0.1% Tween-20) to block nonspecific binding sites. Primary antibodies diluted in 5% skim milk TBS-T were applied to the blot with gentle shaking for 1 hr, at room temperature (anti-caveolin-1 antibody diluted 1:1,000), or for overnight incubation at 4°C (anti-CAR ab2240, 1:1,000 dilution). After extensive washing, diluted secondary antibodies (1:3,000 dilution for both the HRP-conjugated anti-rabbit and anti-mouse antibodies in 5% skim milk, TBS-T) were applied for 1 hr at room temperature with gentle shaking and detected using the SuperSignal Substrate (Pierce Biotechnology, Inc., Rockford, IL) as per the manufacturer's instructions. Chemiluminescence was detected using a cooled charge-coupled device (CCD) camera attached to an imaging capture system (Gene-Gnome; Syngene, Frederick, MD). SDS-PAGE and Western blotting of the lipid raft fractions were also performed as above with equal volumes of each fraction loaded onto the gel.

For indirect immunofluorescence, transduced U87 cells were grown on poly-L-lysine-treated 12 mm coverslips for 2 days in standard DMEM supplemented with 10% FBS. Immunofluorescence on live unpermeabilized cells was performed by incubating the cells with 50 μl of polyclonal anti-CAR ab2240 at 1:500 dilution in DMEM supplemented with 10% FBS at 4°C for 2 hr. After three 10 min washes (0.14 M NaCl, 0.1% Tween-20 in PBS, pH 7.3), the cells were fixed with 4% paraformaldehyde in PBS containing 4% sucrose (pH 7.3) for 15 min at room temperature. Nonspecific sites were blocked in a blocking solution containing 5% BSA + 5% goat normal serum in PBS for 30 min at room temperature. Fifty microliters of Alexa Fluor 555-conjugated secondary antibody diluted to 1:250 in blocking solution was then laid

on top of the coverslip for 30 min at room temperature. After three 10 min washes with wash buffer, the stained cells were analyzed in a Leica wide-field fluorescence microscope under oil immersion objective (×100). The same exposure time was used for all of the samples. The images were processed using Openlab software.

Lipid raft fractionation

Detergent-free fractionation of lipid raft-enriched microdomains was performed as described.[31] The modified lipid raft fractionation scheme replaces the detergent Triton X-100 with sodium carbonate, which detaches peripheral membrane proteins. Briefly, cultured cells were washed twice with ice-cold PBS and scraped into 2 ml of ice-cold Na_2CO_3 (500 mM in double-distilled water, pH 11) solution supplemented with protease inhibitors (complete, mini, EDTA-free protease inhibitor cocktail tablet; Roche Diagnostics Canada, Laval, Quebec) and membranes were disrupted into fine fragments by Dounce homogenization (tight fitting, 15 strokes), followed by sonication on ice (three 20 sec bursts with 10 sec rests in between). Two milliliters of the homogenate was then mixed with an equal volume of 90% (w/v) sucrose in MES buffered solution (MBS) (25 mM morpholinoethanesulfonic acid (MES), 150 mM NaCl, pH 6.5) and placed beneath a 5–35% discontinuous sucrose gradient (4 ml of 5% sucrose/4 ml of 35% sucrose, both in MBS containing 250 mM Na_2CO_3) in an ultracentrifuge tube. The samples were centrifuged at 260,000*g* in a Beckman ultracentrifuge with a SW40 Ti rotor for 16–20 hr at 4°C. Due to their low buoyant density, lipid raft-enriched membranes will float up to the 5–35% sucrose interface and be concentrated there while the cytosolic and high-density membrane fragments will remain at the bottom of the tube. A total of 13 equal-volume fractions (1 ml each, with the 13th fraction being the pellet fraction) were taken from the top of the sucrose gradient to the bottom, and an equal volume was reconstituted in 1× SDS-sample buffer and analyzed by SDS-PAGE and Western blotting for CAR and lipid raft markers such as caveolin-1, as described above.

Three-dimensional spheroid assay

Spheroids of each of the transduced U87 cell lines were generated by spinner cultures, and spheroids of similar diameter were selected and encased in a collagen type I gel as described.[32] Briefly, transduced U87 cells in monolayer culture were trypsinized and seeded into spinner culture flasks at approximately 4×10^6 cells/100 ml DMEM with 10% FBS and spun at 180 rpm for 2 weeks, at which time spheroids of similar diameter were implanted into collagen type I gel (600 μl per well, Vitrogen 100, purchased from Cohesion Technologies, Palo Alto, CA) in 24-well plates. The gel was then overlaid with 500 μl of DMEM supplemented with 10% FBS. The medium was changed every 3 days. Each day for 10 days, cell invasion was assessed with the aid of an inverted microscope. Invasion distance was calculated as the distance in micrometers from the spheroid edge to the most distant population of invasive cells. The experiment was repeated with 3 different preparations of spheroids.

Tumor implantation

Stereotactic injections were performed as described in Li *et al.*[33] CD1 *nu/nu* athymic nude mice (6 weeks old, Charles River Canada, St-Constant, Quebec) were anesthetized by i.p. injection of sodium pentobarbital (25 mg/kg) and placed in a stereotactic apparatus (Kopf). A burr hole was drilled 1 mm anterior and 2 mm lateral to the bregma. The transduced U87 cell suspension (1×10^5 cells in 3 μl of Hank's balanced salt solution (HBSS) was injected stereotactically over a 10 min period using a Hamilton syringe at a depth of 3.5 mm. After 39 days, the animals were euthanized and the tumor volumes analyzed as described below. All animal experimentation was carried out according to the guidelines of the Canadian Council on Animal Care. After euthanasia, brains were removed and quick frozen in isopentane chilled with liquid nitrogen. Coronal sections (10 μm) were prepared and stained for nuclei with hematoxylin alone or for CAR also with an anti-CAR N-terminal (ab2240) or an anti-CAR C-terminal (abRP291) antibody. The secondary anti-rabbit antibody was conjugated to horseradish peroxidase and revealed by DAB reaction. Three-dimensional reconstruction of tumors was performed as described[33] on 10 μm thick sections that were mounted on glass slides and stained for nuclei. Tumor volumes were calculated using the formula $a \times b^2 \times 0.4$, in which a represents the longest axis and b represents the width perpendicular to this axis.

Statistical analysis

All values reported are expressed as means ± SEM. Statistical analyses were performed with Prism software (Graph Pad). Statistical significance was assessed by Student's *t*-test or ANOVA as stated in the figures. Statistical significances were defined as $p < 0.05$.

Results

Like several other human glioma cell lines,[23–27] the U87-MG cells do not express detectable levels of endogenous CAR (Fig. 1). To study the effect of CAR expression on glioma biology, the cells were infected with retroviral vectors carrying transgenes encoding the full-length mCAR1 isoform and the tailless CAR (CAR781) with a deleted cytoplasmic domain (except for the first 2 cytoplasmic juxtamembrane amino acids) (Fig. 1). All experiments were performed with the respective pooled clonal populations in order to avoid heterogeneity between different, isolated clonal lines. The transduced cell populations expressed robust levels of full-length CAR and the tailless CAR as determined by Western blot analysis using a polyclonal antibody against the extracellular domain of CAR (ab2240). Immunoreactivity was absent in the control cells infected with empty vector (U87LNCX). Immunolabeling of live, unpermeabilized cells at 4°C revealed punctate membrane staining (Fig. 2), demonstrating that the exogenous CAR was targeted to the cell surface; the full-length and tailless CAR were distributed similarly (Fig. 2).

We also compared the susceptibility to adenovirus infection of the different cell populations by infecting them with an AdVlacZ at various multiplicities of infection (MOIs) (Fig. 3). At all MOIs tested, both U87CAR and U87CAR-tailless cells had significantly higher infection efficiency than the U87LNCX cells, indicating that the exogenous cell surface CAR proteins are functional as adenovirus receptors. At the highest MOI, only a 2-fold difference was observed between the infectibility of the 3 cell populations.

CAR has been reported to localize to a novel lipid-rich microdomain: after detergent-free extraction, it colocalizes with lipid raft markers such as caveolin-1, but after Triton X-100 treatment, it is found in the heavy, nonlipid raft, clathrin-associated fraction.[31] During fractionation of the cell lysates under detergent-free conditions, both full-length CAR and the tailless CAR (Fig. 4*a*) colocalized with the lipid raft marker caveolin-1. Very little CAR immunoreactivity was found in the higher-density nonlipid raft fractions, indicating that in U87-MG cells most of the exogenously expressed CAR fractionates into lipid-rich domains.

To determine whether CAR expression affected the growth rate of the glioma cell populations in serum-supplemented (10% FBS) or serum-reduced (0.2% FBS) conditions, cell proliferation was determined over the course of 6 days. No significant difference was observed between the growth patterns of the 3 different cell populations (Fig. 5*a* and *b*), suggesting that expression of either the full-length CAR or the tailless CAR had no effect on the growth rate of the glioma cells in monolayer cultures.

Next, using a spheroid model, we compared the invasive behavior of U87CAR, U87CAR-tailless and U87LNCX in a 3-dimensional environment. Spheroids of each cell population were generated by spinner cultures, and spheroids of similar diameter were encased in a collagen type I gel as described.[32] In this model, the cells of the spheroid first lose contact with the spheroid bulk and then invade the collagen gel. When the total invasion distance was measured as a

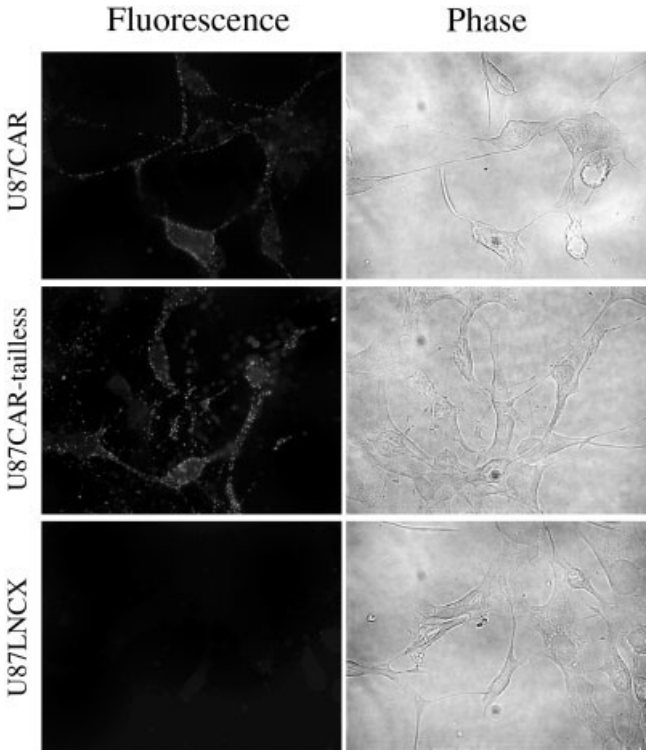

FIGURE 2 – Cell surface localization of CAR. Live, unpermeabilized cells were incubated at 4°C with anti-CAR antibody (ab2240) followed by Alexa fluor 555-conjugated secondary antibodies. Immunofluorescent staining of the extracellular domain of CAR could be observed on U87CAR and U87CAR-tailless cells, while U87LNCX cells exhibited no staining. The corresponding phase contrast images are shown on the right. Images were taken under ×100 oil immersion objective.

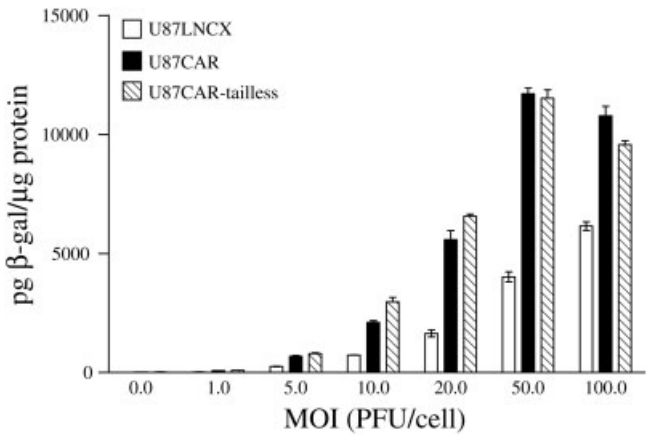

FIGURE 3 – Adenoviral transducibility of the different U87-MG cell populations. Cells were infected with an adenovirus expressing the *E. coli* β-galactosidase gene (AdVlacZ) at various MOIs (pfu/cell). The efficiency of adenoviral infection was quantified through assay of β-galactosidase enzyme activity by luminometry.[8] The light units were converted to picograms of β-galactosidase using a standard curve established with pure β-galactosidase enzyme, and the results are expressed as picograms of β-galactosidase enzyme/microgram of input protein. Note that at all MOIs, U87CAR and U87CAR-tailless showed similar extents of transducibility.

function of time, the U87CAR cells migrated away from the bulk of the spheroids a significantly shorter distance than the control U87LNCX cells (Fig. 6*a*). In contrast, there was no difference between the U87CAR-tailless and the control U87LNCX cells (Fig. 6*b*). These results suggest that expression of CAR retards the invasive behavior of the glioma spheroids and that this effect is dependent on the presence of the cytoplasmic domain of CAR.

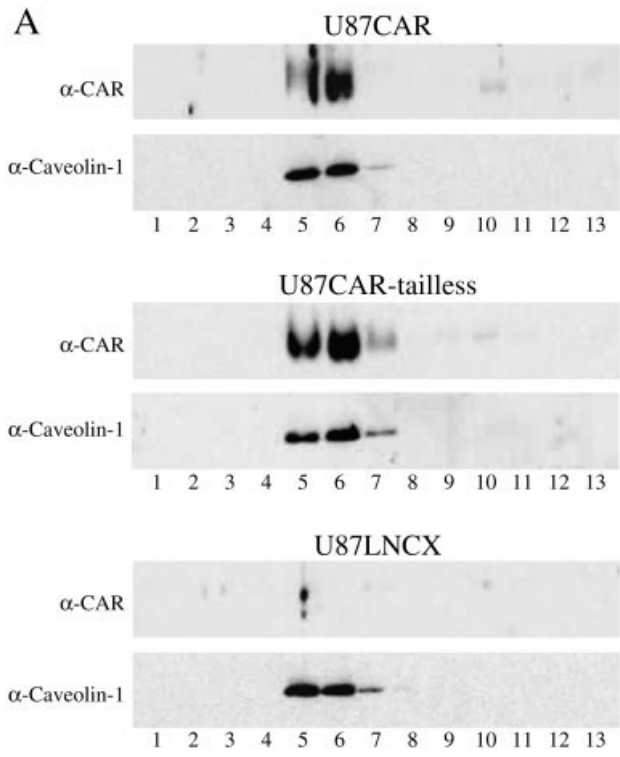

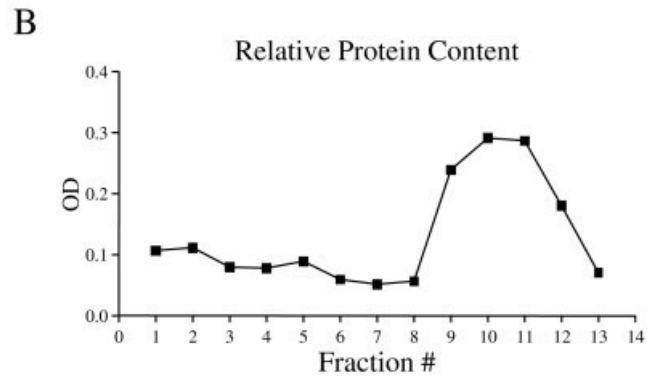

FIGURE 4 – Distribution of CAR during lipid raft fractionation. *(a)* U87-MG cell populations were extracted with Na_2CO_3 solution followed by sucrose gradient fractionation. Equal-volume fractions were taken from the top to the bottom of the tube (fraction 1 is the top fraction and fraction 13 is the bottom fraction), and equal volumes of the fractions were analyzed by Western blotting for CAR (with anti-CAR N-terminal antibody 2240) and caveolin-1 (a marker used for lipid raft and caveolae fractions). *(b)* The protein content of the fractions was determined by BCA assay and expressed as OD readings. A typical protein content profile is shown.

To further study the effect of CAR expression on glioma cells, we determined the *in vivo* growth of each cell population after intracerebral implantation in immunodeficient mice. Three-dimensional reconstruction of the established tumor was performed[33] to calculate volumes of the tumors induced by U87CAR and U87CAR-tailless cells (Table I) and compared to those induced by the U87LNCX control cells. The U87CAR cells generated significantly smaller tumors than the control U87LNCX cells, whereas the tumor sizes were similar

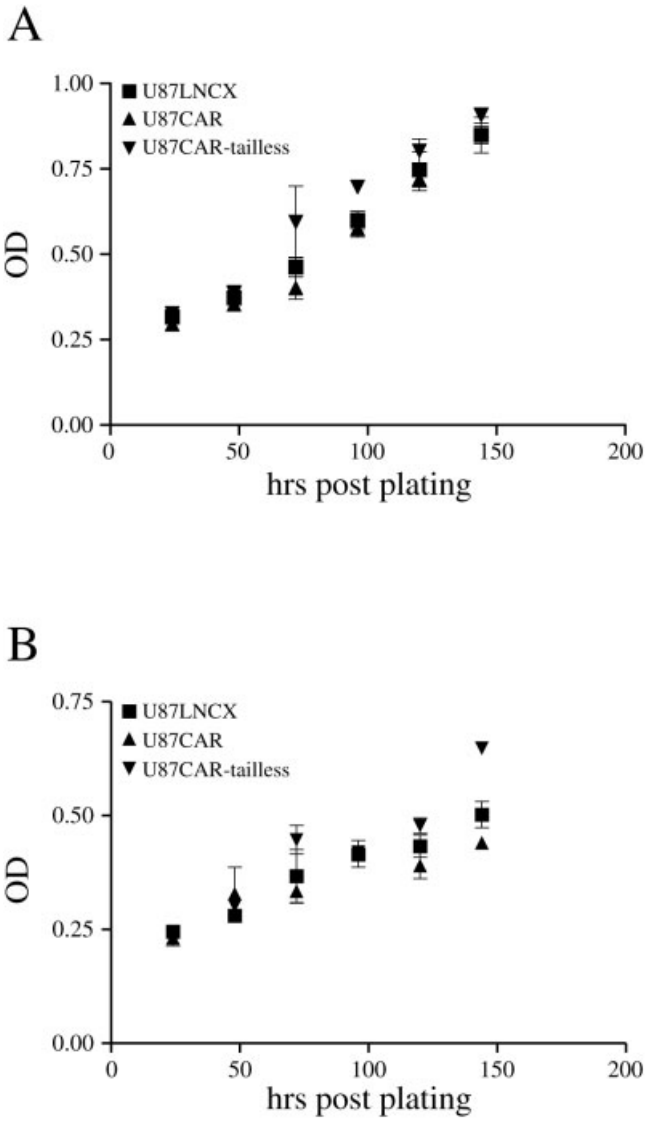

FIGURE 5 – Cell proliferation assays. The different U87-MG cell populations were seeded in microtiter plates in serum (10% FBS)-supplemented medium *(a)* or serum-reduced (0.2% FBS) medium *(b)* as described in Material and Methods. At the indicated times, XTT proliferation assays were performed and spectrophotometric absorbance of the samples was measured as OD. Values represent the mean ± SEM for 3 experiments, $n = 4$ for each experiment, $p > 0.05$ by one-way ANOVA test.

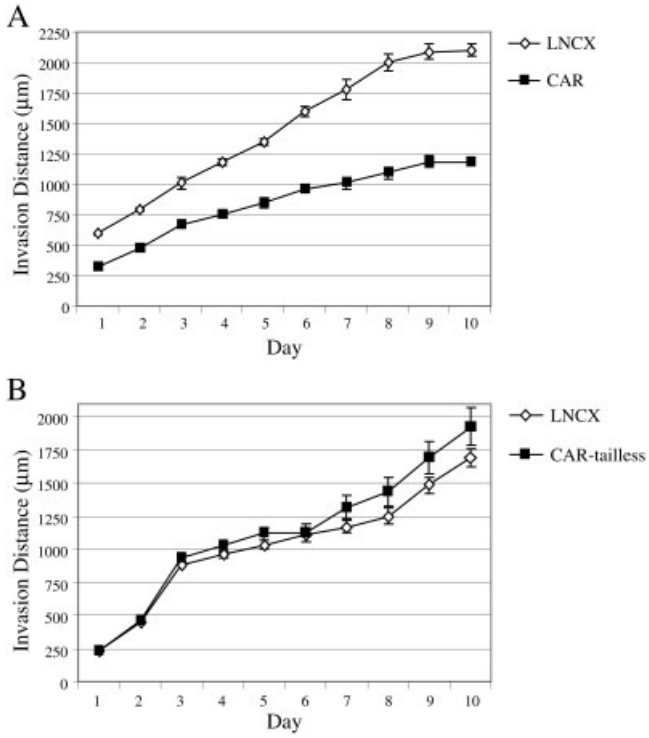

FIGURE 6 – Invasion assay of the different U87-MG cell populations. Spheroids of each of the cell populations were generated by spinner cultures, and spheroids of similar diameter were selected and encased in a collagen type I gel. Each day, for 10 days, cell invasion of the spheroid bulk was assessed with the aid of an inverted microscope. Invasion distances were calculated as the distance in micrometers from the spheroid edge to the most distant population of invasive cells. Shown are representative experiments of invasion distance as a function of time for U87CAR vs. U87LNCX *(a)* and U87CAR-tailless vs. U87LNCX *(b)* spheroids. Values represent the mean ± SEM for one experiment; $n = 9$ for both experiments; each experiment was repeated 3 times. $p < 0.05$ by unpaired *t*-test for U87CAR vs. U87LNCX spheroids. $p > 0.05$ by unpaired *t*-test for U87CAR-tailless vs. U87LNCX spheroids.

TABLE I – INTRACEREBRAL GROWTH OF IMPLANTED CELL POPULATIONS[1]

Cell line	Number	Tumor volume ± S.E. (mm^3)	Duration (days)
U87CAR	N = 15	9.8 ± 4.3[2]	39
U87CAR-tailless	N = 11	37.6 ± 9.2[3]	39
U87LNCX	N = 9	69.2 ± 23.3	39

[1]The differences between the implanted populations was statistically significant by the Kruskal-Wallis test ($p = 0.0014$). –[2]U87CAR vs. U87LNCX ($p < 0.01$, Dunn's multiple comparison test); U87CAR vs. U87CAR-tailless ($p < 0.05$, Dunn's multiple comparison test).–[3]U87CAR-tailless vs U87LNCX ($p > 0.05$, Dunn's multiple comparison test).

between the U87CAR-tailless and U87LNCX cells. Immunohistochemistry using the anti-CAR N-terminus antibody (ab2240) or the anti-CAR C-terminus antibody (RP291) on brain sections revealed that CAR expression was sustained in the tumor mass throughout the *in vivo* growth period (Fig. 7). The sets of tumors generated by U87CAR and U87CAR-tailless cells exhibited CAR staining, while those established by U87LNCX cells exhibited only background staining (Fig. 7). These results indicate that the expression of CAR in glioma cells can lead to a reduction in growth *in vivo* after implantation and that the cytoplasmic domain is required for this growth inhibitory effect.

Discussion

Within the brain, malignant gliomas are characterized by their extensive cell proliferation and migration. Primary astrocytic tumors express variable levels of CAR, with grade II and III tumors having a higher expression level than grade IV tumors.[27] During development, CAR is expressed in progenitors of astrocytes[16] such as radial glia,[34] and its expression is also observed in primary astrocytic cultures from rodent embryonic brain.[35] Therefore, we generated U87-MG glioma cell populations expressing levels of CAR that are comparable to what is observed in normal brain at birth (Fig. 1). Forced expression of CAR did not affect glioma cell growth in monolayer, but had a profound effect on tumor growth *in vivo*. Monolayer and cell suspension culture do not reflect many of the cellular microenvironment conditions present in the tumor

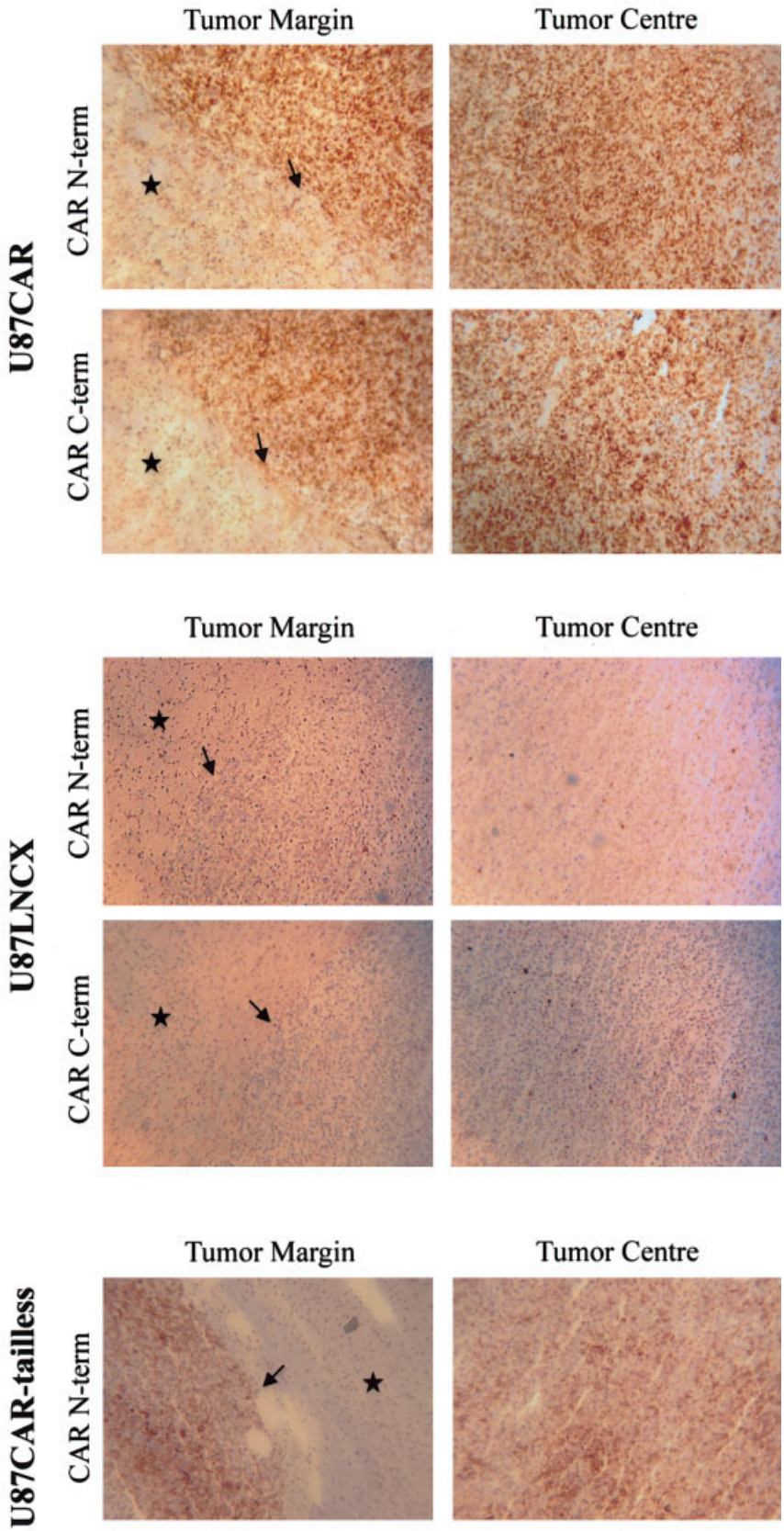

FIGURE 7 – Sustained CAR expression is observed during intracerebral growth of U87CAR (top panel) and U87CAR-tailless (bottom panel) after implantation of the different cell populations. Brain tissue sections were stained for CAR expression with the anti-CAR N-terminal antibody (ab2240) or the anti-CAR C-terminal antibody (RP291). Areas of the tumor margin or tumor center are shown and compared to those of U87LNCX tumors (middle panel). The arrows are pointing to the margin of the tumor mass. The stars are in the brain parenchyma.

mass or the 3-dimensional nature of the extracellular matrix of the brain. For instance, it is known that differences in the microenvironment can have an influence on the 3-dimensional organization, polarity and cytoskeleton of cells,[36,37] as well as affect the expression of matrix-degrading enzymes[36] that are important factors in determining tumor migration and invasion. The need to reconstruct

the 3-dimensional environment encountered by glioma cells *in vivo* to study the effect of CAR expression is also underlined by the finding that growth of epithelial cells within a nonphysiologic microenvironment results in an upregulation of CAR and a shift in the subcellular localization of the protein from cell-cell junctions to cytoplasm.[37] This suggests that the polarity of the 3-dimensional organization of the cell is important in regulating the expression and subcellular localization of CAR, thereby possibly regulating its cellular function. There are many precedents for such behavior, and this disparity between *in vitro* and *in vivo* results is also illustrated by the case of neural CAM (NCAM), which inhibits glioma tumor growth *in vivo* but not *in vitro* in 2-dimensional monolayer cultures.[38,39]

Not only did forced expression of full-length CAR lead to altered *in vivo* growth, but it also affected cell migration and invasion of glioma spheroids. This model reconstructs a first approximation of the rate-limiting breakdown of the 3-dimensional environment that tumor cells must degrade in order to invade.[32] As malignant gliomas invade normal brain by associating with the basement membranes of blood vessels or other basement membrane-like structures that have collagen type I as one of their components,[40–42] our study was carried out with spheroids encased in a gel of collagen type I.[32] It is not clear what caused the marked difference in invasion between the U87CAR and U87LNCX cells. Migration of tumors through a 3-dimensional environment often involves degradation of matrix components by metalloproteases (MMPs).[43] Two of the MMPs that have been implicated in glioma invasiveness are MMP-2 and MMP-9,[44–46] and these have been shown to be regulated by expression of CAMs.[47,48] Gelatin zymography did not show any difference in the levels of MMP-2 or MMP-9, or any other gelatinases, in the 3 cell populations described in our study (data not shown). The transcript levels of the tissue inhibitors of MMPs, TIMP-1 to TIMP-4, were also not changed between the cell populations (data not shown). CAR expression may affect other proteolytic activities or signaling pathways involved in cell migration.

There was a striking difference between U87CAR and U87CAR-tailless in terms of invasion behavior and *in vivo* growth. Considering the high degree of conservation of the cytoplasmic domain of CAR between species (up to 95% identity between the murine and human CAR homologs)[1,12] and the potential phosphorylation motifs and sorting signal motifs residing in the cytoplasmic domain, it is easily conceivable that CAR's cytoplasmic domain may play an important physiologic function. At the very least, the cytoplasmic domain may mediate protein-protein interactions that can regulate CAR trafficking/microdomain localization as has been suggested for other proteins.[49] Although the immunolocalization and fractionation studies did not reveal any differences in the cellular placement of CAR, all lipid microdomains are not equal,[50,51] and subtle differences in the targeting of exogenous CAR may lead to an inability to interact with the appropriate signaling molecules.[31,52] The requirement of the cytoplasmic domain of CAMs for tumor-suppressive activity is also seen for NCAM. The expression of transmembrane NCAM but not glycosyl phosphatidylinositol (GPI)-anchored NCAM has been found to down-regulate secretion of MMPs in tumor cell lines, despite the ability of both forms of NCAM to mediate cell aggregation,[47] demonstrating that adhesion alone is sometimes not sufficient for CAM function. On the other hand, the D1 Ig domain of CAR seems required for its growth inhibitory effect,[30] indicating that both extracellular and intracellular domains cooperate in providing maximal effect.

In contrast to our results, previous studies have shown that a tailless CAR (containing only the transmembrane portion and the first 2 amino acids, i.e., cysteine-cysteine) has tumor growth inhibitory activity that is similar to that of full-length CAR.[21,30] Considering the fact that deletion of the entire cytoplasmic domain abrogates tumor inhibitory activity,[21,30] it is difficult to understand how inclusion of the cysteine-cysteine sequence would restore this activity. The cysteine-cysteine residues provide an S-acylation motif for modification of CAR with the fatty acid palmitate.[52] Although palmitylation is known to regulate protein localization into lipid rafts, it is not known if palmitylation is required for CAR's localization to lipid microdomains. Although it remains to be seen whether the tailless CAR and full-length CAR are targeted to the same lipid microdomains, our results argue against the misfolding, instability, or mislocalization of tailless CAR.

A possible explanation for the discrepancy may be that most of the other studies were performed with single clonal lines and did not use orthotopic models, but rather relied on subcutaneous injection of tumor cells into the flank of mice. Considering the great physiologic heterogeneity of clonal populations within glioma cell lines,[53] we opted to work with pooled populations of retrovirus-transduced cells. As glioma cell growth and invasion are greatly influenced by the extracellular matrix, implantation of the cell populations within the brain provides a rigorous test of the growth inhibitory activity of CAR.

Acknowledgements

We thank C. Guérin and K. Rostworowski for technical help and Dr. R. del Maestro for advice on spheroids. K.-C.H. was supported by a studentship from FRSQ-FCAR; N.L. is a postdoctoral fellow of aktion benni & co e.V.; and J.N. is a national research scholar of FRSQ and a Killam scholar.

References

1. Bergelson JM, Cunningham JA, Droguett G, Kurt-Jones EA, Krithivas A, Hong JS, Horwitz MS, Crowell RL, Finberg RW. Isolation of a common receptor for coxsackie B viruses and adenoviruses 2 and 5. Science 1997;275:1320–3.
2. Tomko RP, Xu R, Philipson L. HCAR and MCAR: the human and mouse cellular receptors for subgroup C adenoviruses and group B coxsackieviruses. Proc Natl Acad Sci U S A 1997;94:3352–6.
3. Cohen CJ, Shieh JT, Pickles RJ, Okegawa T, Hsieh JT, Bergelson JM. The coxsackievirus and adenovirus receptor is a transmembrane component of the tight junction. Proc Natl Acad Sci U S A 2001;98:15191–6.
4. Fechner H, Haack A, Wang H, Wang X, Eizema K, Pauschinger M, Schoemaker R, Veghel R, Houtsmuller A, Schultheiss HP, Lamers J, Poller W. Expression of coxsackie adenovirus receptor and alphav-integrin does not correlate with adenovector targeting in vivo indicating anatomical vector barriers. Gene Ther 1999;6:1520–5.
5. Pickles RJ, Fahrner JA, Petrella JM, Boucher RC, Bergelson JM. Retargeting the coxsackievirus and adenovirus receptor to the apical surface of polarized epithelial cells reveals the glycocalyx as a barrier to adenovirus-mediated gene transfer. J Virol 2000;74:6050–57.
6. Wang X, Bergelson JM. Coxsackievirus and adenovirus receptor cytoplasmic and transmembrane domains are not essential for coxsackievirus and adenovirus infection. J Virol 1999;73:2559–62.
7. Walters RW, Grunst T, Bergelson JM, Finberg RW, Welsh MJ, Zabner J. Basolateral localization of fiber receptors limits adenovirus infection from the apical surface of airway epithelia. J Biol Chem 1999;274:10219–6.
8. Nalbantoglu J, Pari G, Karpati G, Holland PC. Expression of the primary coxsackie and adenovirus receptor is downregulated during skeletal muscle maturation and limits the efficacy of adenovirus-mediated gene delivery to muscle cells. Hum Gene Ther 1999;10:1009–19.
9. van't Hof W, Crystal RG. Manipulation of the cytoplasmic and transmembrane domains alters cell surface levels of the coxsackie-adenovirus receptor and changes the efficiency of adenovirus infection. Hum Gene Ther 2001;12:25–34.
10. Tallone T, Malin S, Samuelsson A, Wilbertz J, Miyahara M, Okamoto K, Poellinger L, Philipson L, Pettersson S. A mouse model for adenovirus gene delivery. Proc Natl Acad Sci U S A 2001;98:7910–5.
11. Wan YY, Leon RP, Marks R, Cham CM, Schaack J, Gajewski TF, DeGregori J. Transgenic expression of the coxsackie/adenovirus receptor enables adenoviral-mediated gene delivery in naive T cells. Proc Natl Acad Sci U S A 2000;97:13784–9.

12. Bergelson JM, Krithivas A, Celi L, Droguett G, Horwitz MS, Wickham T, Crowell RL, Finberg RW. The murine CAR homolog is a receptor for coxsackie B viruses and adenoviruses. J Virol 1998;72: 415–9.
13. Bruning A, Runnebaum IB. CAR is a cell-cell adhesion protein in human cancer cells and is expressionally modulated by dexamethasone, TNFalpha, and TGFbeta. Gene Ther 2003;10:198–205.
14. Honda T, Saitoh H, Masuko M, Katagiri-Abe T, Tominaga K, Kozakai I, Kobayashi K, Kumanishi T, Watanabe YG, Odani S, Kuwano R. The coxsackievirus-adenovirus receptor protein as a cell adhesion molecule in the developing mouse brain. Brain Res Mol Brain Res 2000;77:19–28.
15. Tomko RP, Johansson CB, Totrov M, Abagyan R, Frisen J, Philipson L. Expression of the adenovirus receptor and its interaction with the fiber knob. Exp Cell Res 2000;255:47–55.
16. Hotta Y, Honda T, Naito M, Kuwano R. Developmental distribution of coxsackie virus and adenovirus receptor localized in the nervous system. Brain Res Dev Brain Res 2003;143:1–13.
17. Li Y, Pong RC, Bergelson JM, Hall MC, Sagalowsky AI, Tseng CP, Wang Z, Hsieh JT. Loss of adenoviral receptor expression in human bladder cancer cells: a potential impact on the efficacy of gene therapy. Cancer Res 1999;59:325–30.
18. Li D, Duan L, Freimuth P, O'Malley BW Jr. Variability of adenovirus receptor density influences gene transfer efficiency and therapeutic response in head and neck cancer. Clin Cancer Res 1999;5:4175–81.
19. Pearson AS, Koch PE, Atkinson N, Xiong M, Finberg RW, Roth JA, Fang B. Factors limiting adenovirus-mediated gene transfer into human lung and pancreatic cancer cell lines. Clin Cancer Res 1999;5: 4208–13.
20. Hemmi S, Geertsen R, Mezzacasa A, Peter I, Dummer R. The presence of human coxsackievirus and adenovirus receptor is associated with efficient adenovirus-mediated transgene expression in human melanoma cell cultures. Hum Gene Ther 1998;9:2363–73.
21. Okegawa T, Pong RC, Li Y, Bergelson JM, Sagalowsky AI, Hsieh JT. The mechanism of the growth-inhibitory effect of coxsackie and adenovirus receptor (CAR) on human bladder cancer: a functional analysis of car protein structure. Cancer Res 2001;61:6592–600.
22. Rauen KA, Sudilovsky D, Le JL, Chew KL, Hann B, Weinberg V, Schmitt LD, McCormick F. Expression of the coxsackie adenovirus receptor in normal prostate and in primary and metastatic prostate carcinoma: potential relevance to gene therapy. Cancer Res 2002;62: 3812–8.
23. Lamfers ML, Grill J, Dirven CM, van Beusechem VW, Geoerger B, Van Den BJ, Alemany R, Fueyo J, Curiel DT, Vassal G, Pinedo HM, Vandertop WP, et al. Potential of the conditionally replicative adenovirus Ad5-Delta24RGD in the treatment of malignant gliomas and its enhanced effect with radiotherapy. Cancer Res 2002;62:5736–42.
24. Miller CR, Buchsbaum DJ, Reynolds PN, Douglas JT, Gillespie GY, Mayo MS, Raben D, Curiel DT. Differential susceptibility of primary and established human glioma cells to adenovirus infection: targeting via the epidermal growth factor receptor achieves fiber receptor-independent gene transfer. Cancer Res 1998;58:5738–48.
25. Mori T, Arakawa H, Tokino T, Mineura K, Nakamura Y. Significant increase of adenovirus infectivity in glioma cell lines by extracellular domain of hCAR. Oncol Res 1999;11:513–21.
26. Asaoka K, Tada M, Sawamura Y, Ikeda J, Abe H. Dependence of efficient adenoviral gene delivery in malignant glioma cells on the expression levels of the coxsackievirus and adenovirus receptor. J Neurosurg 2000;92:1002–8.
27. Fuxe J, Liu L, Malin S, Philipson L, Collins VP, Pettersson RF. Expression of the coxsackie and adenovirus receptor in human astrocytic tumors and xenografts. Int J Cancer 2003;103:723–9.
28. Anders M, Christian C, McMahon M, McCormick F, Korn WM. Inhibition of the Raf/MEK/ERK pathway up-regulates expression of the coxsackievirus and adenovirus receptor in cancer cells. Cancer Res 2003;63:2088–95.
29. Okegawa T, Li Y, Pong RC, Bergelson JM, Zhou J, Hsieh JT. The dual impact of coxsackie and adenovirus receptor expression on human prostate cancer gene therapy. Cancer Res 2000;60:5031–6.
30. Kim M, Sumerel LA, Belousova N, Lyons GR, Carey DE, Krasnykh V, Douglas JT. The coxsackievirus and adenovirus receptor acts as a tumour suppressor in malignant glioma cells. Br J Cancer 2003;88: 1411–6.
31. Ashbourne Excoffon KJ, Moninger T, Zabner J. The coxsackie B virus and adenovirus receptor resides in a distinct membrane microdomain. J Virol 2003;77:2559–67.
32. Tamaki M, McDonald W, Amberger VR, Moore E, Del Maestro RF. Implantation of C6 astrocytoma spheroid into collagen type I gels: invasive, proliferative, and enzymatic characterizations. J Neurosurg 1997;87:602–9.
33. Li H, Alonso-Vanegas M, Colicos MA, Jung SS, Lochmuller H, Sadikot AF, Snipes GJ, Seth P, Karpati G, Nalbantoglu J. Intracerebral adenovirus-mediated p53 tumor suppressor gene therapy for experimental human glioma. Clin Cancer Res 1999;5:637–42.
34. Tamamaki N, Nakamura K, Okamoto K, Kaneko T. Radial glia is a progenitor of neocortical neurons in the developing cerebral cortex. Neurosci Res 2001;41:51–60.
35. Xu R, Mohanty JG, Crowell RL. Receptor proteins on newborn Balb/c mouse brain cells for coxsackievirus B3 are immunologically distinct from those on HeLa cells. Virus Res 1995;35:323–40.
36. Unemori EN, Werb Z. Reorganization of polymerized actin: a possible trigger for induction of procollagenase in fibroblasts cultured in and on collagen gels. J Cell Biol 1986;103:1021–31.
37. Anders M, Hansen R, Ding RX, Rauen KA, Bissell MJ, Korn WM. Disruption of 3D tissue integrity facilitates adenovirus infection by deregulating the coxsackievirus and adenovirus receptor. Proc Natl Acad Sci U S A 2003;100:1943–8.
38. Edvardsen K, Pedersen PH, Bjerkvig R, Hermann GG, Zeuthen J, Laerum OD, Walsh FS, Bock E. Transfection of glioma cells with the neural-cell adhesion molecule NCAM: effect on glioma-cell invasion and growth in vivo. Int J Cancer 1994;58:116–22.
39. Owens GC, Orr EA, DeMasters BK, Muschel RJ, Berens ME, Kruse CA. Overexpression of a transmembrane isoform of neural cell adhesion molecule alters the invasiveness of rat CNS-1 glioma. Cancer Res 1998;58:2020–8.
40. Mahesparan R, Read TA, Lund-Johansen M, Skaftnesmo KO, Bjerkvig R, Engebraaten O. Expression of extracellular matrix components in a highly infiltrative in vivo glioma model. Acta Neuropathol (Berl) 2003;105:49–57.
41. Chintala SK, Gokaslan ZL, Go Y, Sawaya R, Nicolson GL, Rao JS. Role of extracellular matrix proteins in regulation of human glioma cell invasion in vitro. Clin Exp Metastasis 1996;14:358–66.
42. Giese A, Bjerkvig R, Berens ME, Westphal M. Cost of migration: invasion of malignant gliomas and implications for treatment. J Clin Oncol 2003;21:1624–36.
43. Binder DK, Berger MS. Proteases and the biology of glioma invasion. J Neurooncol 2002;56:149–58.
44. Nakano A, Tani E, Miyazaki K, Yamamoto Y, Furuyama J. Matrix metalloproteinases and tissue inhibitors of metalloproteinases in human gliomas. J Neurosurg 1995;83:298–307.
45. Rao JS, Yamamoto M, Mohaman S, Gokaslan ZL, Fuller GN, Stetler-Stevenson WG, Rao VH, Liotta LA, Nicolson GL, Sawaya RE. Expression and localization of 92 kDa type IV collagenase/gelatinase B (MMP-9) in human gliomas. Clin Exp Metastasis 1996;14:12–8.
46. Sawaya RE, Yamamoto M, Gokaslan ZL, Wang SW, Mohanam S, Fuller GN, McCutcheon IE, Stetler-Stevenson WG, Nicolson GL, Rao JS. Expression and localization of 72 kDa type IV collagenase (MMP-2) in human malignant gliomas in vivo. Clin Exp Metastasis 1996;14:35–42.
47. Edvardsen K, Chen W, Rucklidge G, Walsh FS, Obrink B, Bock E. Transmembrane neural cell-adhesion molecule (NCAM), but not glycosyl-phosphatidylinositol-anchored NCAM, down-regulates secretion of matrix metalloproteinases. Proc Natl Acad Sci U S A 1993; 90:11463–7.
48. Maidment SL, Rucklidge GJ, Rooprai HK, Pilkington GJ. An inverse correlation between expression of NCAM-A and the matrix-metalloproteinases gelatinase-A and gelatinase-B in human glioma cells in vitro. Cancer Lett 1997;116:71–7.
49. McCabe JB, Berthiaume LG. N-terminal protein acylation confers localization to cholesterol, sphingolipid-enriched membranes but not to lipid rafts/caveolae. Mol Biol Cell 2001;12:3601–17.
50. Harder T, Simons K. Caveolae, DIGs, and the dynamics of sphingolipid-cholesterol microdomains. Curr Opin Cell Biol 1997;9:534–42.
51. Simons K, Toomre D. Lipid rafts and signal transduction. Nat Rev Mol Cell Biol 2000;1:31–9.
52. van't Hof W, Crystal RG. Fatty acid modification of the coxsackievirus and adenovirus receptor. J Virol 2002;76:6382–6.
53. Carson SD, Pirruccello SJ. Tissue factor and cell morphology variations in cell lines subcloned from U87-MG. Blood Coagul Fibrinolysis 1998;9:539–47.